Structure Characterization of Tetra-PEG Gel by Small-Angle Neutron Scattering

Takuro Matsunaga,[‡,†] Takamasa Sakai,[‡,§] Yuki Akagi,[§] Ung-il Chung,[§] and Mitsuhiro Shibayama*[,†]

The Institute for Solid State Physics, The University of Tokyo, 5-1-5 Kashiwanoha, Kashiwa, Chiba, 277-8581, Japan, and Department of Bioengineering, School of Engineering, The University of Tokyo, 7-3-1 Hongo, Bunkyo-ku, Tokyo 113-8656, Japan

Received October 10, 2008; Revised Manuscript Received January 1, 2009

ABSTRACT: The structure of Tetra-PEG gel, a new class of biocompatible, easy-made, and high-strength hydrogel consisting of a four-arm polyethylene glycol (PEG) network, has been investigated by means of small-angle neutron scattering (SANS). Since the Tetra-PEG gel is prepared by cross-end-coupling two kinds of four-arm PEG macromers having different functional groups at the ends, i.e., amine group and succinimidyl ester group respectively, the coupling reaction occurs exclusively between PEG chains carrying different functional groups. SANS results showed that the four-arm PEG macromer aqueous solutions and Tetra-PEG gels were successfully described by the theoretical scattering function for multiarm Gaussian chains and the Ornstein−Zernike function, respectively. Surprisingly, no noticeable excess scattering that originated from cross-linking was observed in Tetra-PEG gels, suggesting that its network structure is extremely uniform. Investigations on nonstoichiometric Tetra-PEG gels showed weakening of the mechanical properties as well as an increase of dangling chains (defects) in the network. It is concluded that Tetra-PEG gels have an extremely uniform network structure, probably mimicking a diamond-like structure, and this is one of the reasons for the advanced mechanical properties of Tetra-PEG gels.

Introduction

Polymer gels consist of polymer network swollen in water (hydrogels), in oil (lipogels), or in air (aerogels). Because of their high retention capacity of water, oil, and air, polymer gels have been utilized as super absorbent, oil-recovery materials and mechanical absorbers, etc.[1,2] On the other hand, due to low polymer concentrations, most polymer gels have disadvantages in their mechanical properties, which have been limiting their applications. In particular, applications to biomedical materials such as artificial muscle, cartilage, and tendon, which require advanced mechanical properties as well as biocompatibility, have been desired for years.

One of major reasons for insufficient mechanical strength is cross-link inhomogeneities introduced during gel preparation. Cross-link inhomogeneities were found in vulcanized rubbers[3] and in polymer gels.[4] The understanding of cross-link inhomogeneity is very important from both scientific and engineering points of view since it affects the physical properties of the polymer network, such as mechanical and optical properties.[5] Inhomogeneous distribution of cross-links leads to stress-concentration in low cross-link density regions, resulting in mechanical breakdown. In order to circumvent this problem, various types of gels were proposed, such as networks prepared by end-linking of well-defined prepolymers,[6] gels obtained by gamma ray cross-linking of polymer solutions.[7] Recently, several novel gels having advanced mechanical properties are proposed on the basis of completely different concepts, namely slide ring gels,[8] nanocomposite gels,[9] and double network gels.[10] Though these gels meet the criterion of the mechanical properties, other criteria, such as biocompatibility and easy preparation are not satisfied.

Sakai et al. developed a novel class of hydrogels that meet all of these criteria, i.e., high mechanical strength and toughness, easy preparation, and biocompatibility.[11] The gel, called Tetra-PEG gel, consists of two kinds of four-arm polyethylene glycol (PEG) macromers of the same size, tetraamine-terminated PEG (TAPEG) and tetra-NHS-glutarate-terminated PEG (TNPEG). Here, NHS represents for *N*-hydroxysuccinimide. By mixing TAPEG and TNPEG aqueous solutions, Tetra-PEG gel can be instantaneously formed not only in laboratory but also in vivo. The mechanical properties are remarkably high (of the order of a few to tens MPa for the strength at break for 120 mg/mL Tetra-PEG gel made of 10 kDa macromers), being comparable to those of native articular cartilage (approximately 6−10 MPa). Tetra-PEG gel seems to have an extremely homogeneous network structure with very low degrees of defects in the network. However, the structure−property relationship has not been fully elucidated. In this paper, we extensively studied the network structure of Tetra-PEG gel as well as the structure of precursor macromers, i.e., TAPEG and TNPEG, in aqueous solutions using small-angle neutron scattering (SANS).

Theoretical Background

1. Thermodynamics of Polymer Solutions and Gels. In the context of Flory−Huggins theory for polymer solutions,[12] the osmotic pressure of the polymer solution is given by

$$\Pi = -\frac{RT}{V_1}\left[\ln(1-\phi) + \left(1-\frac{1}{z}\right)\phi + \chi\phi^2\right] \quad (1)$$

where V_1 is the molar volume of the solvent, R is the gas constant, T is the absolute temperature, ϕ is the volume fraction of the polymer, and χ is the Flory−Huggins interaction parameter. z is the reduced degree of polymerization of the solute polymer normalized to the molar volume of the solvent, V_1.

$$z = \left(\frac{V_2}{V_1}\right)Z \quad (2)$$

Here, Z is the degree of polymerization of the polymer based on the monomer unit of the polymer and V_2 is the molar volume

* To whom correspondence should be addressed. E-mail shibayama@issp.u-tokyo.ac.jp.
† The Institute for Solid State Physics, The University of Tokyo.
‡ These authors contributed equally to the work.
§ Department of Bioengineering, School of Engineering, The University of Tokyo.

10.1021/ma802280n CCC: $40.75
Published on Web 02/03/2009

of the monomeric unit of the solute (polymer). The osmotic modulus is given by[13]

$$K_{os} = \phi\frac{\partial\Pi}{\partial\phi} = \frac{RT\phi}{V_2 Z}\left[1 + \left(\frac{1}{1-\phi} - 2\chi\right)\left(\frac{V_2}{V_1}\right)\phi Z\right] \quad (3)$$

Note that the factor (V_2/V_1) is necessary for the case where the molar volume of the monomeric unit of the solute is different from that of the solvent.

In the case of polymer gels, there are two contributions to the osmotic pressure. One is from the free energy of mixing, Π_{mix}, and the other is from the elasticity of network chains, Π_{el}. Since the degree of polymerization is infinite ($z \rightarrow \infty$ or $Z \rightarrow \infty$) for gels, Π_{mix} is given by taking $z \rightarrow \infty$ in eq 1, i.e.

$$\Pi_{mix} = -\frac{RT}{V_1}[\ln(1-\phi) + \phi + \chi\phi^2] \quad \text{(polymer gel)} \quad (4)$$

On the other hand, Π_{el} is obtained by[14]

$$\Pi_{el} = \nu_e RT\left[\frac{1}{2}\left(\frac{\phi}{\phi_0}\right) - \left(\frac{\phi}{\phi_0}\right)^{1/3}\right] \quad (5)$$

where ν_e is the number density of the effective elastic chains in the network and ϕ_0 is the volume fraction of the polymer at preparation. At swelling equilibrium, the following equation holds:[15]

$$\Pi = \Pi_{mix} + \Pi_{el} = 0 \quad (6)$$

Hence, ν_e is obtained for affine-model networks

$$\nu_{e,aff} = \frac{[\ln(1-\phi) + \phi + \chi\phi^2]}{V_1\left[\frac{1}{2}\left(\frac{\phi}{\phi_0}\right) - \left(\frac{\phi}{\phi_0}\right)^{1/3}\right]} \quad \text{(affine)} \quad (7)$$

This is the so-called Flory−Rehner equation and is used to determine the cross-link density (or the number density of effective polymer chains in a polymer network).[14] In the case of phantom chains, the number density of effective polymer chains is modified to[16]

$$\nu_{e,ph} = \nu_{e,aff}\left(1 - \frac{2}{f_x}\right) \quad (8)$$

where f_x is the functionality of the cross-link. Since the phantom network does not have the translational entropy term of cross-links, the equation for swelling equilibrium is given by[17]

$$\nu_{e,ph} = -\frac{[\ln(1-\phi) + \phi + \chi\phi^2]}{V_1\left(\frac{\phi}{\phi_0}\right)^{1/3}} \quad \text{(phantom)} \quad (9)$$

for the $f_x = 4$ network. The phantom chain model allows that fluctuations of the displacement of cross-links after deformation are equal to those of undeformed state and are given by $\langle(\Delta\mathbf{r})^2\rangle = \langle(\Delta\mathbf{r})^2\rangle_0 = 2\langle\mathbf{r}^2\rangle_0/f_x$.[18] Here, $\mathbf{r}$ and $\Delta\mathbf{r}$ denote the end-to-end distance of polymer chains between neighboring cross-inks and its deviation from the affine deformation, respectively, and the subscript 0 means undeformed state. This leads to $\langle(\Delta\mathbf{r})^2\rangle = \langle(\Delta\mathbf{r})^2\rangle_0 = \langle\mathbf{r}^2\rangle_0/2$ for $f_x = 4$, which is too large for Tetra-PEG gels as will be discussed later. Hence, we employ the affine model hereafter.

The osmotic modulus of polymer gels is given by

$$K_{os} = K_{os,mix} + K_{os,el} = \frac{RT\phi^2}{V_1}\left(\frac{1}{1-\phi} - 2\chi\right) + \nu_e RT\left[\frac{1}{2}\left(\frac{\phi}{\phi}\right) - \frac{1}{3}\left(\frac{\phi}{\phi_0}\right)^{1/3}\right] \quad (10)$$

The longitudinal modulus is obtained by[19]

$$M_{os} = K_{os} + \frac{4}{3}G \quad (11)$$

Here, G is the shear modulus given by[13]

$$G = \nu_e RT\left(\frac{\phi}{\phi_0}\right)^{1/3} \quad (12)$$

Hence,

$$M_{os} = K_{os} + \frac{4}{3}G = \frac{RT\phi^2}{V_1}\left(\frac{1}{1-\phi} - 2\chi\right) + \nu_e RT\left[\frac{1}{2}\left(\frac{\phi}{\phi_0}\right) + \left(\frac{\phi}{\phi_0}\right)^{1/3}\right] \quad (13)$$

2. The Scattering Intensity Functions for Star-Polymer Solutions and Polymer Gels. According to the Einstein's fluctuation theory,[20] the scattering intensity at $q = 0$ (i.e., the thermodynamic limit), $I(0)$, for polymer solutions is related to the osmotic modulus by

$$I(0) = (\Delta\rho)^2\frac{k_B T\phi^2}{K_{os}} \quad (14)$$

where q is the magnitude of the scattering vector and $(\Delta\rho)^2$ is the scattering length density difference square between the polymer (2) and solvent (1) given by

$$(\Delta\rho)^2 = (\rho_2 - \rho_1)^2 = \left[\left(\frac{b_2}{\tilde{V}_2}\right) - \left(\frac{b_1}{\tilde{V}_1}\right)\right]^2 \quad (15)$$

Here, b_i and $\tilde{V}_i$ are the scattering length and the monomeric volume of component i (=1 or 2). Since $I(0)$ is related to eq 3, the scattering intensity function for polymer−solvent systems is given by the single-contact theory of Zimm:[21,22]

$$I(q) = \frac{(\Delta\rho)^2}{N_A}\frac{V_2\phi P_{star}(q)}{1 + (1-2\chi)\left(\frac{V_2}{V_1}\right)\phi P_{star}(q)} \quad (16)$$

Here, N_A is the Avogadro's number, and ϕ is the volume fraction of the solute. $P_{star}(q)$ is the form factor of f-arm star-polymer chains given by[23,24]

$$P_{star}(q) = \frac{2Z}{fu^2}\left\{u - [1 - \exp(-u)] + \frac{f-1}{2}[1 - \exp(-u)]^2\right\} \quad (17)$$

where f is the number of arms of the star polymer and $u \equiv Za^2q^2/6$. Note that

$$P(0)_{star} = \frac{Z}{f} + \frac{(f-1)Z}{f} = Z \quad (18)$$

The radius of gyration of the star polymer, $R_{g,star}$ is related to that of the arm polymer by

$$R^2_{g,star} = \frac{(3f-2)}{f}R^2_{g,arm} = \frac{(3f-2)}{f^2}\frac{Za^2}{6} \quad (19)$$

The scattering function for polymer gels is given as a sum of the Ornstein−Zernike function (OZ)[25] and a squared-Lorentzian function (SL) as written by[26,27]

$$I(q) = \frac{(\Delta\rho)^2 RT\phi^2}{N_A M_{os}}\left[\frac{1}{1+\xi^2q^2} + \frac{A_{inhom}}{(1+\Xi^2q^2)^2}\right] \quad (20)$$

Here, ξ is the correlation length of the network and Ξ is the characteristic size of inhomogeneities in the gel. A_{inhom} is a constant representing the contribution of frozen inhomogeneities and is independent of q. It is known that the OZ function

represents thermal concentration fluctuations and the SL term represents frozen-spatial inhomogeneities. Since M_{os} is given by eq 13, $I(0)$ for polymer gels is given by

$$I(0) = \frac{(\Delta\rho)^2\phi^2}{N_A}\frac{1}{\frac{\phi^2}{V_1}\left(\frac{1}{1-\phi}-2\chi\right)+\nu_e\left[\frac{1}{2}\left(\frac{\phi}{\phi_0}\right)+\left(\frac{\phi}{\phi_0}\right)^{1/3}\right]}[1+A_{inhom}] \quad (21)$$

Experimental Section

Sample Preparation. Tetraamine-terminated PEG (TAPEG) and tetra-NHS-glutarate-terminated PEG (TNPEG) were prepared from tetrahydroxyl-terminated PEG (THPEG) having equal arm lengths. The details of TAPEG and TNPEG preparation are reported elsewhere.[11] The molecular weights (M_w) of TAPEG and TNPEG were matched to be either 10 k or 20 kDa. Here, NHS represents for *N*-hydroxysuccinimide. The activity of the functional group was estimated using NMR. Tetra-PEG gels were synthesized as follows. Constant amounts of TAPEG and TNPEG (5−160 mg/mL) were dissolved in phosphate buffer (pH7.4) and phosphate-citric acid buffer (pH5.8), respectively. In order to control the reaction rate, the ionic strengths of buffers were chosen to be 25 mM for lower macromer concentrations (5−100 mg/mL) and 75 mM for higher macromer concentrations (110−160 mg/mL). Two solutions were mixed and the resulting solution was poured into the mold. At least 12 h was spent for completion of reaction before the following experiments. No noticeable sol fraction was detected by NMR. SANS samples were prepared in quartz cell with equi-amounts (stoichiometric case) or with different compositions (nonstoichiometric case) of Tetra-PEG-10k and Tetra-PEG-20k. Note that the condition of sample preparation was significantly changed from that employed in the previous paper.[11] The pHs were carefully chosen so as not to cause hydrolysis and to optimize the coupling reaction. The gelation time was also extended from 4 to 12 h for completion of coupling reaction. The initial macromer concentrations were varied from 5 to 160 mg/mL. The corresponding initial polymer volume fractions, ϕ_0, were in the range between 4.43×10^{-3} and 1.42×10^{-1}.

Mechanical and Swelling Measurements. Stretching measurements were carried out for rectangular-shaped films (30 mm high, 5 mm wide, and 2 mm thick) of Tetra-PEG gel using a mechanical testing apparatus (RHEO METER:CR-500DX-SII, Sun Scientific Co.) at a velocity of 0.1 mm/sec. Shear experiments were also conducted for disk shape films 25 mm in diameter and 1 mm in thickness using dynamic viscoelasticity measuring apparatus (MCR301, Anton Paar.) In the case of swelling measurements, sample specimens of the same size as those for the stretching measurements were immersed in large amount of deionized water for at least 2 days. Then, the weights of the specimens were measured in order to calculate the polymer fraction in equilibrium swelling state.

Small-Angle Neutron Scattering (SANS). Small-angle neutron scattering experiments were carried out at two-dimensional SANS instrument, SANS-U, the University of Tokyo, located at JRR-3 Research Rector, Japan Atomic Energy Agency, Tokai, Ibaraki, Japan. Monochromated cold neutron beam with the average neutron wavelength of 7.00 Å and 10% wavelength distribution was irradiated to the samples. The scattered neutrons were counted with a two-dimensional position detector (Ordela 2660N, Oak Ridge, USA). The sample-to-detector distance was chosen to be 1 and 4 m for macromer measurements and 2 and 8 m for Tetra-PEG measurements. After necessary corrections for open beam scattering, transmission and detector inhomogeneities, the corrected scattering intensity functions were normalized to the absolute intensity scale with a polyethylene secondary standard. The details of the instrument are reported elsewhere.[28,29] Incoherent scattering subtraction was made by fitting the observed scattering functions with eq 16 or OZ functions by taking account of the method reported by Shibayama et al.[30]

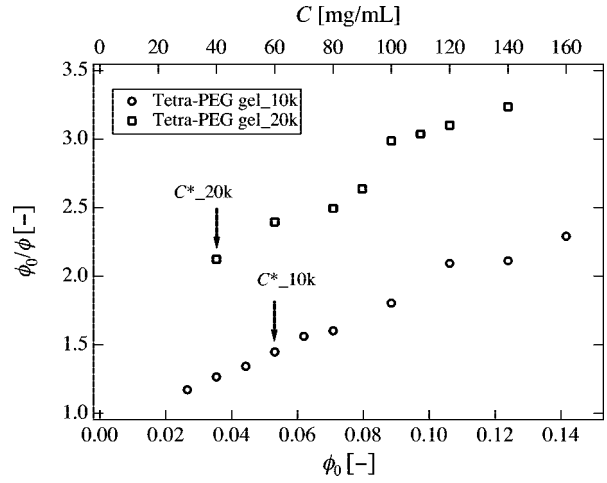

Figure 1. Initial polymer volume fraction, ϕ_0, dependence of the swelling degrees, ϕ_0/ϕ, for Tetra-PEG-10k and Tetra-PEG-20k. The up-arrow and down-arrow indicate the chain overlap concentrations for Tetra-PEG-10k and Tetra-PEG-20k, respectively evaluated by viscometry.

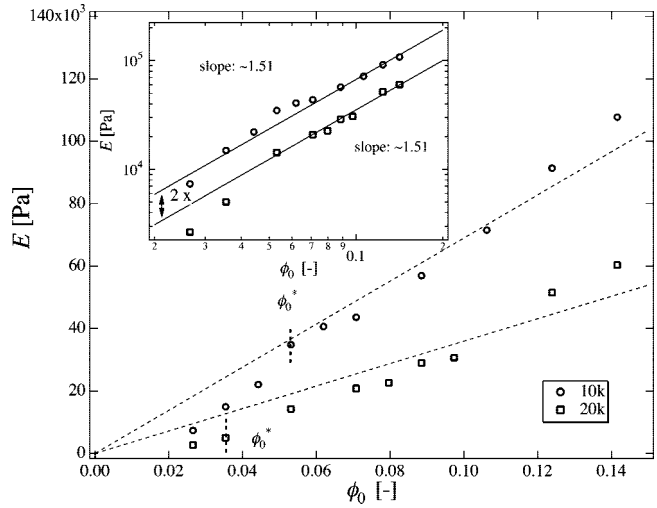

Figure 2. ϕ_0 dependence of Young's moduli, E, for Tetra-PEG-10k and Tetra-PEG-20k. The dashed lines are fitted lines by crossing the origin and by fitting the data for $\phi_0 \gg \phi_0^*$. The inset shows the log−log plots.

Results and Discussion

1. Swelling and Mechanical Properties. Figure 1 shows the swelling degree, ϕ_0/ϕ, as a function of ϕ_0 for Tetra-PEG-10k and Tetra-PEG-20k. Here, ϕ_0 is the polymer volume fraction at sample preparation. The degree of swelling increases approximately linearly with ϕ_0. The higher the initial polymer concentration, the larger the degree of swelling is. Note that (1) ϕ_0/ϕ is in the range of 1 to 3, and (2) a uniform gel was prepared from a solution of Tetra-PEG-10k even with a half of the so-called C^* concentration evaluated by viscometry, C^* (≈60 mg/mL), i.e., 30 mg/mL ($\phi_0 = 2.26 \times 10^{-2}$).[11] This indicates that network formation occurs by spontaneous chain-stretching and coupling of succinimidyl ester and amine groups at chain ends. In the case of Tetra-PEG-20k, a gel prepared with the concentration lower than C^* was too brittle to measure the swelling ratio.

Figure 2 shows the variation of Young's modulus, E, as a function of ϕ_0 for Tetra-PEG-10k and of Tetra-PEG-20k. We also measured the shear modulus, G, and confirmed the relationship, $E \approx 3G$ (valid for materials with Poisson ratio being 1/2). According to eq 12, E is expected to scale as $E \sim G \sim \nu_e$

$\sim \phi_0$. The dashed lines are drawn by crossing the origin and by fitting with the data for $\phi_0 \gg \phi_0^*$. As a matter of fact, E seems to scale with ϕ_0^1 at high ϕ_0 regions, while E does not cross the origin but reduces to zero by approaching ϕ_0^*. This is why E depends on ϕ_0 with a higher exponent than unity in the low ϕ_0 region as shown in the inset, i.e., $E \sim \phi_0^{1.51}$. Larger exponents than unity are reported in the literature, e.g., 1.83 for poly(diethylsiloxane) networks.[31] Such a higher exponent is explained as a result of entanglements. However, in the case of Tetra-PEG gels, it is important to note that E is essentially proportional to ϕ_0, indicating absence of entanglements. Note that E's for the two samples are colinear in the log−log plot with the factor of 2 as expected (i.e., $\nu_{e,10k} = 2\nu_{e,20k}$).

It is noteworthy that the order of E is a few tens of kPa, which is about 1 order of magnitude larger than that of typical gels with similar polymer concentrations[32,33] and that of tetra-arm PEG gels made with bifunctional chain extender.[34] Lutolf and Hubbell investigated tetra-arm-PEG gels with 10 and 20 kDa. Their PEG gels were prepared from vinyl sulfonated tetra-arm PEG by Michael-type addition of thiol-containing peptides. Hence, the latter plays as a chain extender. In their case, the order of shear modulus, G, was a few kPa in the concentration range of 5 to 20 w/v%.[34] The origin of the high mechanical strength in Tetra-PEG gels results from its high yield of network formation. The linear relationship between E and ϕ_0 indicates that there are no noticeable entanglements in the network. Therefore, the higher modulus of Tetra-PEG gels is ascribed solely to a high efficiency of network formation with no or very low amount of defects. We conjecture that the superiority in the mechanical properties of Tetra-PEG gels is due to its unique sample preparation, i.e., A−B type end-coupling of tetra-arm PEG. In the following, we further report on the structures of the prepolymer (macromer) solutions and Tetra-PEG gels.

Figure 3 shows the comparison of the number densities of effective polymer chains for (a) Tetra-PEG-10k and (b) Tetra-PEG-20k, evaluated from stoichiometry ($\nu_{e,st}$), swelling equilibrium (affine model; $\nu_{e,aff}$), and mechanical measurements ($\nu_{e,el}$). The stoichiometric number density, $\nu_{e,st}$, is evaluated via

$$\nu_{e,st} = \frac{f_x}{2}\frac{\phi_0}{V_2 Z} = \frac{2\phi_0}{V_2 Z} \tag{22}$$

Here, we set $f_x = f = 4$ and $V_2 = 39.02$ cm^3/mol (monomeric molar mass = 44.04 g, mass density = 1.129 g/cm^3). The ϕ_0 dependence of $\nu_{e,st}$ is shown with a dashed line, The open circles denote $\nu_{e,aff}$. The value of $\chi = 0.43$ was taken from the literature.[34] However, in order to match the values of the number densities from the swelling and mechanical measurements (open squares), it was necessary to play with χ. We fitted the swelling results using affine model with $\nu_{e,el}$ by changing χ as a floating parameter. The best fit was achieved when $\chi = 0.475$ as shown with solid circles ($\nu_{e,aff}$) and open squares ($\nu_{e,el}$). Hence, the experimental χ value in Tetra-PEG gels for the swelling measurements was slightly larger than the value written in the literature. Figure 3b shows the similar plots for Tetra-PEG-20k. Phenomenological equations for $\nu_{e,el}$ obtained by fitting for the limited concentration range are given in the figures, i.e.,

$$\nu_{e,el} = 113\phi_0 - 1.96 \text{ [mol/m}^3\text{]} \quad \text{(Tetra-PEG-10k)}$$

$$\nu_{e,el} = 64.0\phi_0 - 1.75 \text{ [mol/m}^3\text{]} \quad \text{(Tetra-PEG-20k)}$$

These phenomenological equations also indicate no or negligible entanglements in Tetra-PEG gels.

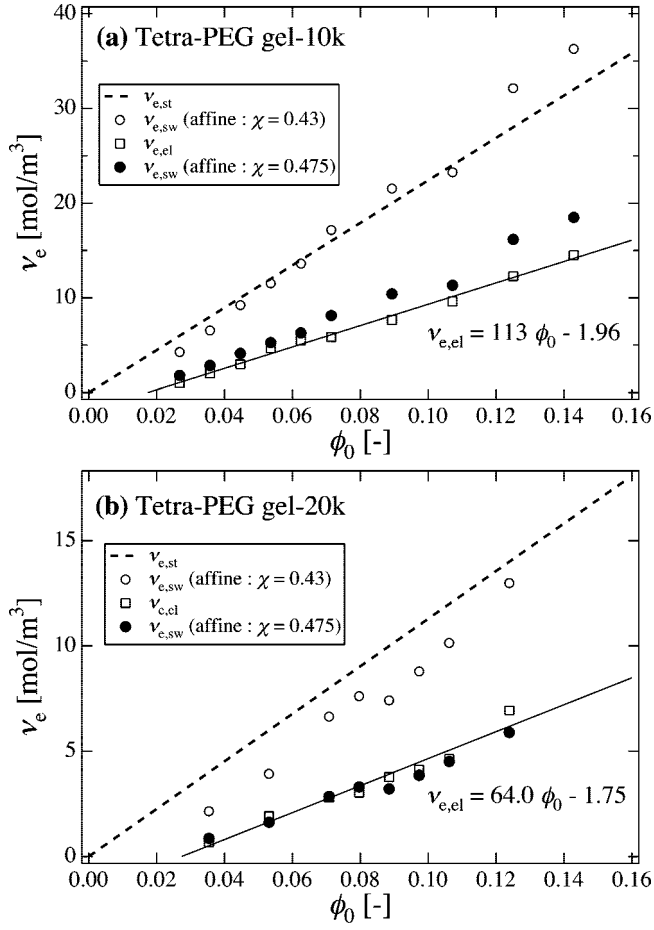

Figure 3. ϕ_0 dependence of the number densities of the effective polymer chains for (a) Tetra-PEG-10k and (b) Tetra-PEG-20k, evaluated from stoichiometry, ($\nu_{e,st}$; dashed line), affine model ($\nu_{e,aff}$; open circles), and Young's modulus ($\nu_{e,el}$; open squares). The solid lines are obtained for $\nu_{e,el}$ as a linear function of ϕ_0.

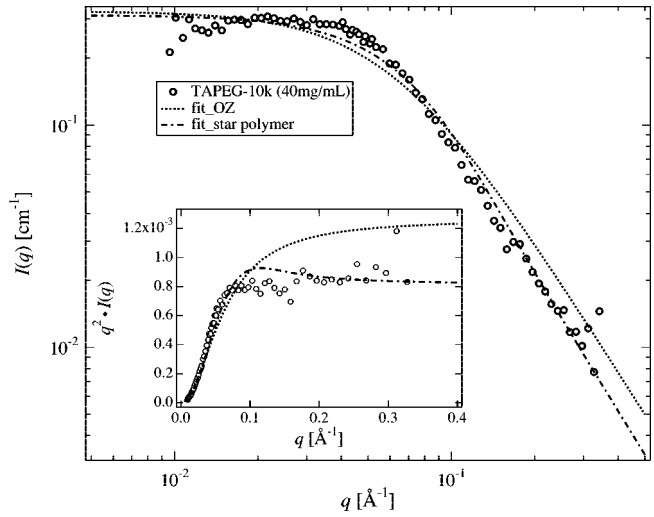

Figure 4. Scattering intensity function of TAPEG-10k macromer aqueous solution. The concentration was 40 mg/mL. The dashed and dotted lines are the fits with the scattering functions of star polymers and of gels, respectively.

2. Tetra-PEG Macromers. Before discussing the structure of Tetra-PEG gels, let us discuss the structure of Tetra-PEG macromers. Figure 4 shows the SANS intensity function, $I(q)$, for TAPEG-10k in deuterated solution. The concentration was $\phi_0 = 3.54 \times 10^{-2}$ (40 mg/mL), which is the one of the lowest concentrations investigated in this work. The dashed and chain lines represent the theoretical scattering functions calculated with the star-polymer (eqs 16 and 17 with $f = 4$ and $\chi = 1/2$) and OZ functions (eq 20 with $A_{inhom} = 0$), respectively. As shown in the figure, the observed scattering function is not well

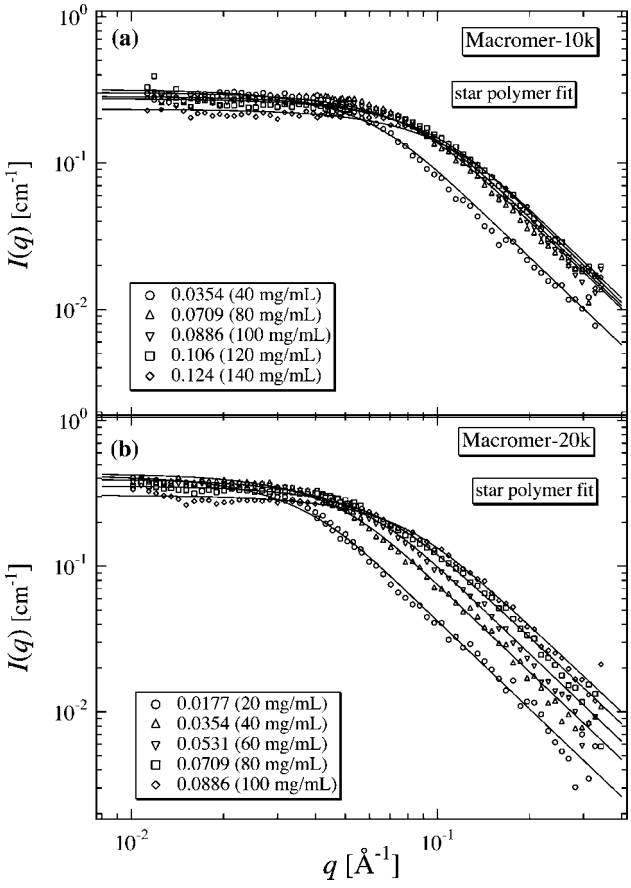

Figure 5. SANS intensity functions of TAPEG macromer solutions (a) TAPEG-10k and (b) TAPEG-20k. The solid lines are obtained by fitting with eq 16.

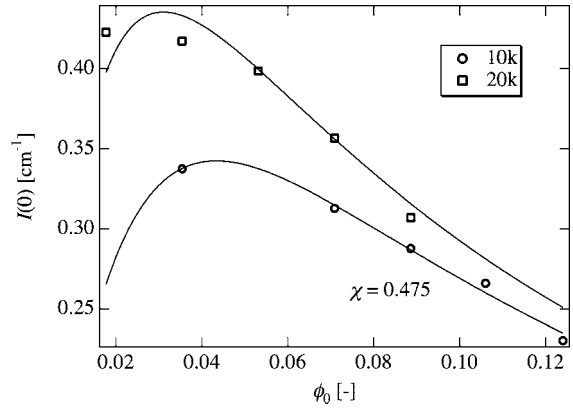

Figure 6. Variation of $I(0)$ as a function of ϕ_0. The solid lines are obtained with eq 16.

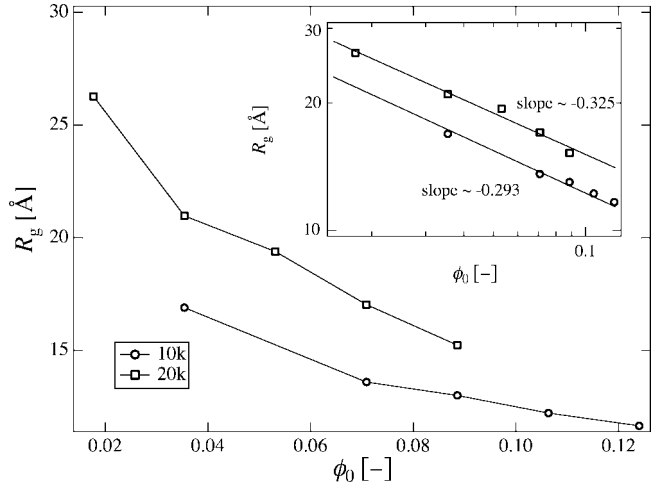

Figure 7. Variation of R_g as a function of ϕ_0. The inset is log−log plot of the same data.

reproduced by the OZ function, but by the star-polymer function. The difference is more clearly seen in the Kratky plot, i.e., $q^2I(q)$ vs q, in the inset.

Figure 5 shows $I(q)$s for (a) TAPEG-10k and (b) TAPEG-20k at various polymer concentrations. $I(q)$s look monotonously decreasing functions of q. $I(0)$ is expected to be proportional to ϕ_0, i.e., $I(0) \sim \phi_0 Z$, if no interpolymer chain interaction exists (i.e., $\chi \approx 1/2$). However, it was found that $I(q)$s did not change systematically as a function of ϕ_0 and were decreasing function of ϕ_0 as shown in Figure 6. As a matter of fact, concentration dependence of $I(0)$ has a peak, and such phenomenon was first reported by Debye and Bueche in turbidity of polymer solutions.[35] Soni and Stein also observed a peak in light scattering intensity for end-linked poly(dimethylsiloxane) solutions.[36] The presence of the maximum in $I(0)$ vs ϕ_0 plot suggests the importance to take into account of the interpolymer chain interaction. The solid lines in Figure 5 were calculated by using eq 16, which takes into account of the interpolymer chain interactions with $\chi = 0.475$. Accordingly, the solid lines in Figure 6 were also calculated with eq 16 with the same parameters.

Figure 7 shows the variations of $R_{g,star}$ for TAPEG-10k and TAPEG-20k as a function of ϕ_0. Note that $R_{g,star}$ is defined as the radius of gyration of the star polymer. Figure 7 indicates that $R_{g,star}$ is a decreasing function of ϕ_0 both for TAPEG-10k and TAPEG-20k. The value of $R_{g,star}$ was 19.1 Å for 40 mg/mL-TAPEG-10k. The hydrodynamic radius of four-arm TAPEG-10k at 10 mg/mL was obtained by dynamic light scattering (DLS). The value was $R_h = 24.2$ Å.[11] By knowing the segment length of PEG chains to be 5.89 Å,[37] the radius of gyration can be estimated via eq 19. The theoretical value is 28.6 Å for the four-arm polymer in Θ condition. The ratio $\rho = R_g/R_h$ is 1.18. This value is reasonably in accordance to the theoretical ratio $\rho = R_g/R_h = 1.333$ (for $f = 4$ star polymer in Θ condition)[38] by considering that the latter is for the Θ condition. However, the values of R_g obtained by SANS are significantly lower than that obtained by DLS and do not satisfy the relation. This is partially due to the difference in the concentrations, i.e., 40 mg/mL (SANS) and 10 mg/mL (DLS). By extrapolating ϕ_0 to 8.86×10^{-3} (10 mg/mL), one obtains $R_{g,star} = 25.4$ Å, which is still below the expected value by the unperturbed chain calculation and by DLS. The reason is not clear at this stage. Apart from the absolute values of $R_{g,star}$, $R_{g,star}$ decreases roughly with a power-law fashion, i.e., $R_{g,star} \sim \phi_0^{\beta}$, with $\beta = -0.293$ (Tetra-PEG-10k) and -0.325 (Tetra-PEG-20k). This indicates that Tetra-PEG macromer solutions consist of space-filled blobs of Tetra-PEG macromers and behave as $R_{g,star} \sim \phi_0^{-1/3}$.

3. Tetra-PEG Gel. Figure 8 shows SANS intensity curves for (a) Tetra-PEG-10k (b) Tetra-PEG-20k at various polymer concentrations. The solid lines represent fitting curves with OZ functions (eq 20)[39] with $A_{inhom} = 0$ and the dashed lines are obtained with the star-polymer function (eq 16). Surprisingly, all the curves for gels are nicely fitted with the theoretical function (eq 20) without the inhomogeneitiy term (i.e., $A_{inhom} = 0$).

Figure 9 shows plots of $I(q)/\phi_0\xi^2$ vs ξq. All the curves for gels are superimposed to a single master curve for (a) Tetra-PEG-10k and (b) Tetra-PEG-20k, respectively. This indicates that all the samples are in semidilute regime where macromer chains are connected to each other and form an infinite network. It should be noted here that the scattering intensity functions

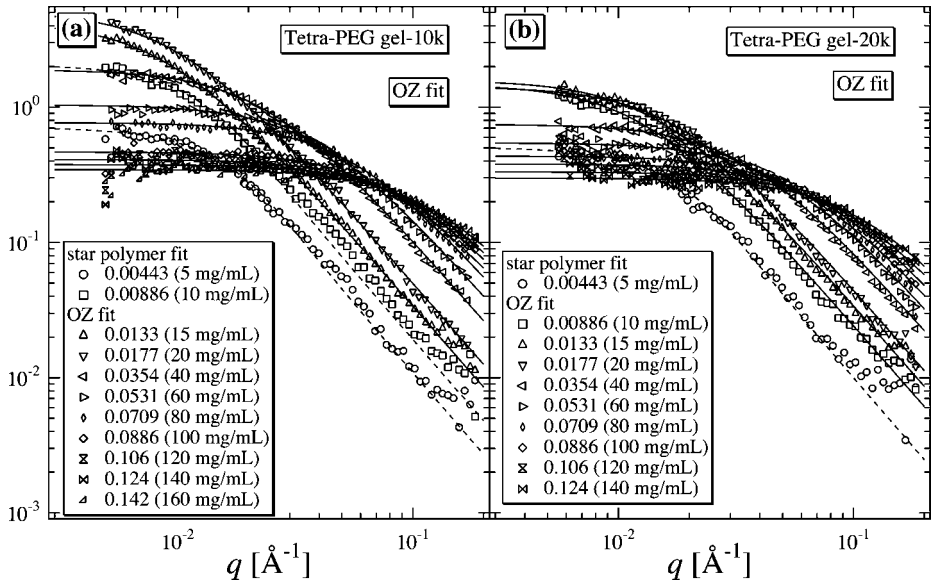

Figure 8. SANS intensity functions of Tetra-PEG gels. (a) Tetra-PEG −10k and (b) Tetra-PEG-20k. The solid lines are obtained by fitting with eq 20 with $A_{\text{inhom}} = 0$. The dashed lines are fitted functions with eq 16 for imperfect gels prepared at low macromer concentrations.

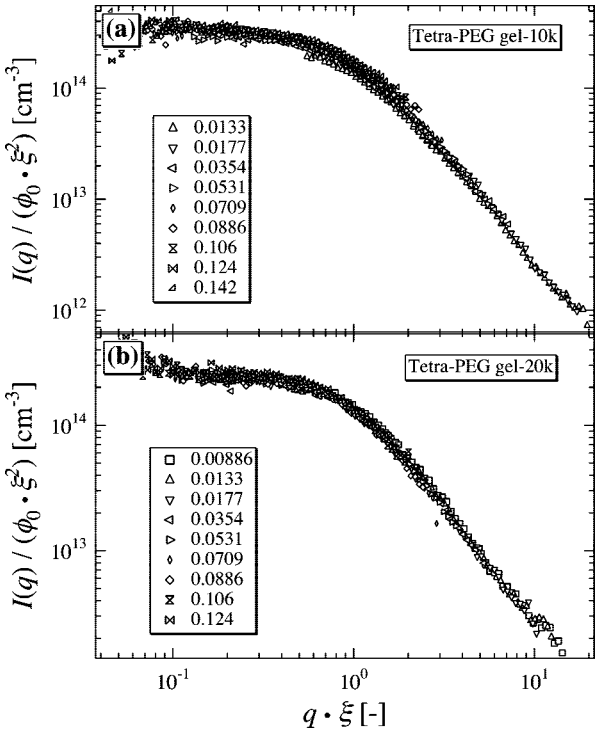

Figure 9. Master curve of Figure 8 for (a) Tetra-PEG−10k and (b) Tetra-PEG–20k.

for polymer gels, in general, cannot be represented by a simple OZ function and hence cannot be superimposed by a single function, such as $I(q)/\phi\xi^2$ vs ξq. Such nonuniversality in the scattering function is ascribed to the contribution of frozen-inhomogeneities (i.e., $A_{\text{imhom}} \neq 0$).[26,40] The experimental results for Tetra-PEG gels, however, strongly suggest that the network structure in Tetra-PEG gels is extraordinarily uniform at least up to the lower bound of the SANS experiment, i.e., 0.003 Å^{-1} (≈2000 Å). It is known that frozen-inhomogeneities appear not in as-prepared gels but in swollen or deformed gels.[26,41] From this point of view, Figure 9 does not fully prove that Tetra-PEG gels have extraordinarily uniform networks. However, Figures 1 and 2 show that gelation in Tetra-PEG occurs even at lower concentrations than ϕ_0*, probably via spontaneous stretching and coupling of the arm chains of TAPEG and

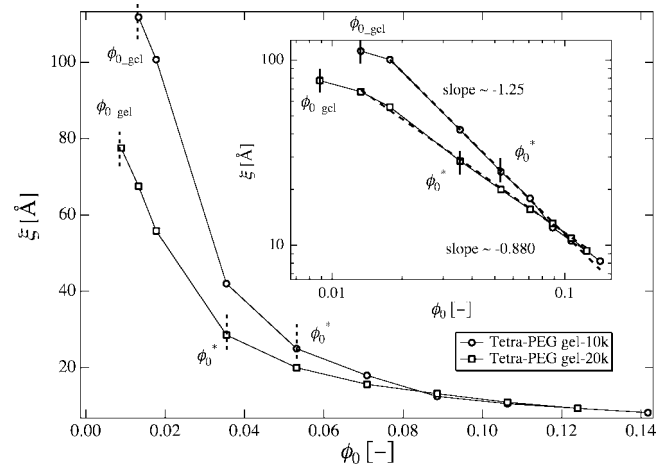

Figure 10. Variation of ξ as a function of ϕ_0. The inset is the log−log plot.

TNPEG. In other words, uniform Tetra-PEG gels are also obtained even from a macromer mixture with $\phi_0 < \phi_0$* and these gel do not have the inhomogeneity term in the SANS function. These data strongly support our argument. Furthermore, we recently carried out SANS measurements for swollen Tetra-PEG gels and observed absence of the inhomogeneity term. The details of the swollen gel systems will be reported in the forthcoming paper. In a more condensed and entangled system, Beltzung et al. reported SANS results on end-linked poly(dimethylsiloxane) network in swelling equilibrium.[6] They also observed no significant increase in scattering intensity. But in the field of hydrogels, Tetra-PEG gel is the first hydrogel having no inhomogeneities in equilibrium swollen state. It should be also mentioned that dynamic light scattering results showed nonergodicity in Tetra-PEG gels.[11] The presence of nonergodicity, in spite of high homogeneity in Tetra-PEG gels, may be ascribed to the fact that nonergodicity is not related to inhomogeneities but to topological fixation of chain motion by cross-linking. This issue will be also addressed in a forthcoming paper.

The variation of correlation length, ξ, is plotted against ϕ_0 in Figure 10. ξ is a decreasing function of ϕ_0. Note that the chain overlap concentrations, ϕ_0*, of the macromer solutions, i.e., TAPEG and TNPEG, are calculated to be around 5.31×10^{-2}

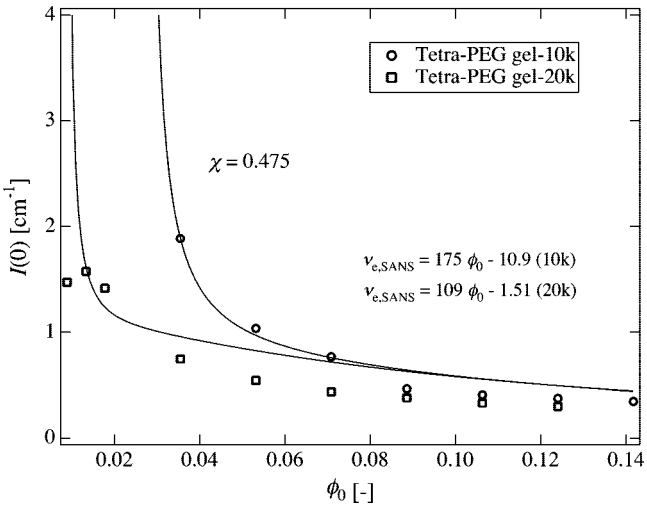

Figure 11. Variation of $I(0)$ as a function of ϕ_0. The solid lines are obtained with eq 21, where the ϕ_0 dependence of χ and ν_e are taken into account.

(60 mg/mL) and 3.54×10^{-2} (40 mg/mL) (marked with arrows) for Tetra-PEG-10k and Tetra-PEG-20k, respectively. If the concentration fluctuations in Tetra-PEG gels are the same as those in polymer solutions in a good solvent, ξ scales as $\xi \sim \phi_0^{-3/4}$ in a good solvent[39] and $\xi \sim \phi_0^{-1}$ in a Θ solvent. Therefore, the exponents shown in the inset, -1.25 (Tetra-PEG-10k) and -0.88 (Tetra-PEG-20k) may indicate that the blob chains in Tetra-PEG gels behave more likely as Gaussian chains than self-avoiding chains. This, in turn, means that the χ parameter of Tetra-PEG gels is close to 1/2.

Figure 11 shows $I(0)$ vs ϕ_0 for Tetra-PEG-10k and Tetra-PEG-20k. $I(0)$ is a decreasing function of ϕ_0, except for the low ϕ_0 region ($\phi_0 < \phi_{0,gel}$). The solid lines are the theoretical functions for $I(0)$ (eq 21) with $A_{inhom} = 0$, with χ evaluated from the SANS analysis on the star-polymer solutions (Figure 5). These lines roughly reproduce the variation of $I(0)$ with ϕ_0, suggesting the validity of the SANS analysis.

The results and discussion given above suggest that the network structure of Tetra-PEG gels is quite uniform and does not have noticeable defects, such as loops and dangling chains. In order to confirm these results more specifically, we carried out SANS experiments for nonstoichiometric cases.

4. Nonstoichiometric Tetra-PEG Gel. According to the discussion given above, it is of particular importance to match the concentration of TAPEG and TNPEG for achieving optimal mechanical properties of Tetra-PEG gels. In order to examine this conjecture, we carried out SANS and mechanical testing experiments for nonstoichiometric Tetra-PEG gels that were prepared with nonstoichiometric compositions, r = [TAPEG]/[TNPEG].

Figure 12a shows SANS intensity curves of Tetra-PEG-10k gels with TAPEG:TNPEG = 100:100 (matched) ($r = 1$), 90:110 ($r = 0.82$), 75:125 ($r = 0.60$), and 50:150 ($r = 0.33$). Interestingly, $I(q)$ is a sensitive function of the degree of asymmetry and decreases progressively when the degree of asymmetry increased. The SANS curve of the macromer (TAPEG) is also shown in the figure. The solid lines are the fits with

$$I(q) = \alpha I_{OZ}(q) + (1 - \alpha) I_{star}(q) \tag{23}$$

Here, α is the ratio of the gel component. The physical meaning of eq 23 is that the minor component is able to couple with the same amount of the other component and forms a network, while the rest of the major component remains as star macromer chains. Curve fitting gives $\alpha = 0.65$ when $r = 0.9$. This means

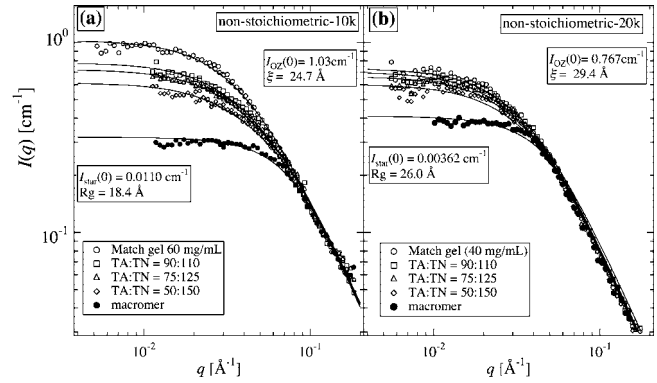

Figure 12. SANS intensity functions of nonstoichiometric Tetra-PEG gels: (a) Tetra-PEG-10k and (b) Tetra-PEG-20k. The solid lines are obtained by fitting with eq 23.

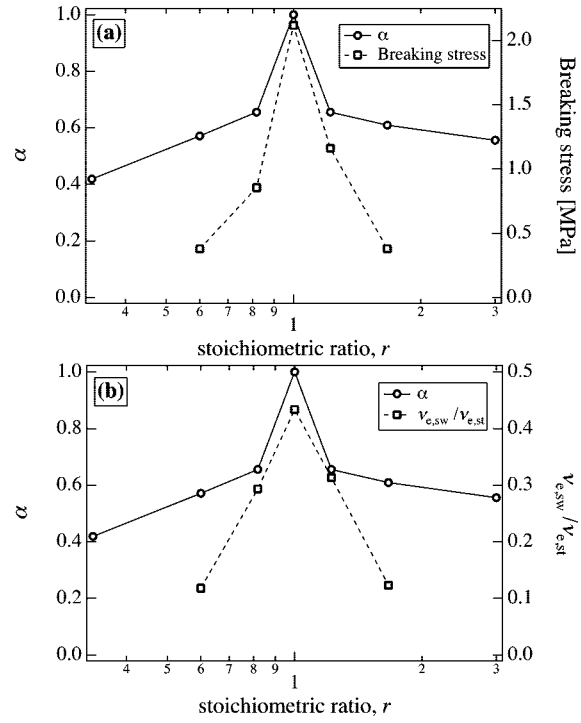

Figure 13. Plots of the ratio of gel component, α (solid line), as a function of the stoichiometric ratio, r. The right axes are (a) the breaking stress and (b) the ratio, $\nu_{e,sw}/\nu_{e,st}$. The χ value for $\nu_{e,sw}$ is 0.475.

that simple additivity does not hold in $I(q)$. A similar result was obtained for the other side of nonstoichiometry, i.e., TAPEG:TNPEG = 110:90 ($r = 1.22$), 125:75 ($r = 1.67$), and 150:50 ($r = 3.0$). It is clear that $I(q)$ decreased when the degree of stoichiometry increased. Figure 12b shows the cases of Tetra-PEG-20k, resulting in the same conclusion as the case of Tetra-PEG-10k.

Figure 13 shows α together with (a) the breaking stress by compression and (b) the number density ratio of effective polymer chains contributing to the elasticity, $\nu_{e,w}/\nu_{e,st}$ as a function of log$r$. As clearly seen, both are symmetric function of log$r$. Figure 13 shows that (1) $I(q)$ and E are strong functions of the degree of stroichiometry and it becomes a maximum at $r = 1$, (2) a slight offset of composition results in a significant deviation from the simple additivity rule of $I(q)$, and (3) the nonmatched TAPEG or TNPEG chains behave as defects of the network, resulting in significant depression of the mechanical properties.

Figure 14 shows schematic models of (a) Tetra-PEG macromer solutions and (b) Tetra-PEG gels as a function of ϕ_0.

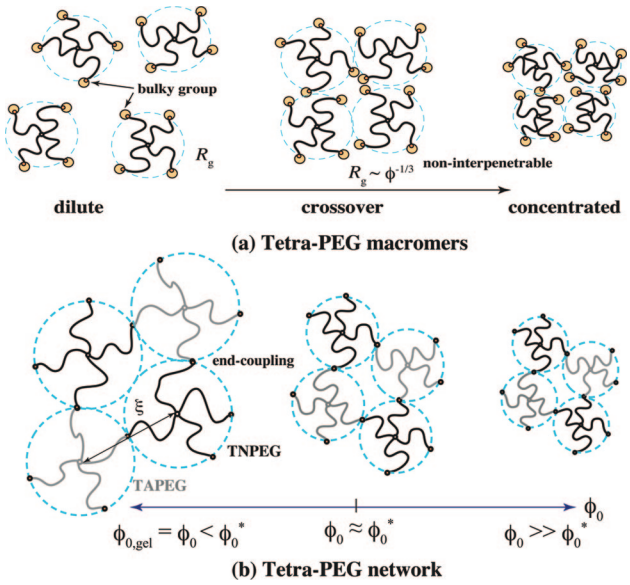

Figure 14. Schematic models showing the concentration-dependence of (a) macromer solutions and (b) Tetra-PEG gels. Due to the presence of bulky/hydrophobic groups at the end of arm chains, macromers are noninterpenetrable even at $\phi_0 > \phi_0^*$. By end-coupling of the end-groups exclusively between TAPEG and TNPEG, a regularly arranged Tetra-PEG gel is formed with a diamond-like architecture.

Due to the presence of a bulky end-group (NHS-glutarate group for TNPEG) or electrostatic repulsive interaction between protonated trimethyleneamine groups for TAPEG at the end of arm chains, macromers do not overlap each other even at a concentration higher than ϕ_0^*. This leads to a formation of Tetra-PEG gels with a low degree of entanglements. Exclusive cross-end-coupling between amino and carboxyl groups of TAPEG and TNPEG macromers enables a formation of a tetrahedron-type network with a high yield and an extremely low degree of defects. All of these natures originating from a unique design of Tetra-PEG gels result in a formation of high-performance biocompatible gels with advanced mechanical properties.

Conclusion

Structure analyses of Tetra-PEG gels were carried out by means of swelling experiments and SANS, and the results were discussed by taking into account the mechanical properties of the same systems. The following facts are disclosed. (1) Tetra-PEG gels are stoichiometrically prepared irrespective of the initial polymer concentration, and their swelling behaviors are well predicted by the Flory−Rehner theory. (2) The mechanical moduli of Tetra-PEG gels, E and G, are proportional to the initial polymer concentration and is 1 order of magnitude larger than the corresponding gels made with similar tetra-arm PEG gels prepared with a low-molecular-weight coupling reagent. This indicates that cross-end-coupling of A- and B-type tetra-PEG is essential for gel preparation with extremely low defects. (3) The scattering functions of the macromers can be well reproduced by the scattering function for star polymers. (4) SANS functions of Tetra-PEG gels can be described by simple Ornstein−Zernike function without excess scattering component originating from cross-linking inhomogeneities. This means that Tetra-PEG gels are extremely homogeneous, and an "ideal" network free from defects is formed. (5) Preparation in nonstoichiometric composition leads to formation of defects in the polymer chain network and results in a significant depression of the mechanical properties. Structural models of macromer solutions and of Tetra-PEG gels, which account for the advanced mechanical properties of Tetra-PEG gels, are proposed.

Acknowledgment. This work was partially supported by the Ministry of Education, Science, Sports and Culture, Japan (Grants-in-Aid for Scientific Research (A), 2006−2008, No. 18205025, and for Scientific Research on Priority Areas, 2006−2010, No. 18068004). The SANS experiment was performed with the approval of Institute for Solid State Physics, The University of Tokyo, at Japan Atomic Energy Agency, Tokai, Japan No. 8615.

References and Notes

(1) de Rossi, D.; Kajiwara, K.; Osada, Y.; Yamauchi, A. *Polymer Gels*; Plenum Press: New York, 1991.000
(2) Osada, Y.; Kajiwara, K. *Gel Handbook*; Academic Press: New York, 2001.000
(3) Stein, R. S. *J. Polym. Sci.* **1969**, *B7*, 657–660.
(4) Bueche, F. *J. Colloid Interface Sci.* **1970**, *33*, 61–66.
(5) Shibayama, M.; Takata, S.; Norisuye, T. *Physica A* **1998**, *249*, 245–252.
(6) Beltzung, M.; Herz, J.; Picot, C. *Macromolecules* **1983**, *16*, 580–584.
(7) Norisuye, T.; Masui, N.; Kida, Y.; Shibayama, M.; Ikuta, D.; Kokufuta, E.; Ito, S.; Panyukov, S. *Polymer* **2002**, *43*, 5289–5297.
(8) Okumura, Y.; Ito, K. *Adv. Mater.* **2001**, *13*, 485–487.
(9) Haraguchi, K.; Takehisa, T. *Adv. Mater.* **2002**, *14*, 1120–1124.
(10) Gong, J. P.; Katsuyama, Y.; Kurokawa, T.; Osada, Y. *Adv. Mater.* **2003**, *15*, 1155–1158.
(11) Sakai, T.; Matsunaga, T.; Yamamoto, Y.; Ito, C.; Yoshida, R.; Suzuki, S.; Sasaki, N.; Shibayama, M.; Chung, U. *Macromoleules* **2008**, *41*, 5379–5384.
(12) Flory, P. J. *Principles of Polymer Chemistry.* Cornell Univ.: Ithaca, NY, 1953.000
(13) Onuki, A. *Adv. Polym. Sci.* **1993**, *109*, 63–121.
(14) Flory, P. J.; Rehner, J., Jr. *J. Chem. Phys.* **1943**, *11*, 521.
(15) Shibayama, M.; Tanaka, T. *Adv. Polym. Sci.* **1993**, *109*, 1–62.
(16) James, H. M.; Guth, E. *J. Chem. Phys.* **1947**, *15*, 669–683.
(17) Mark, J. E.; Erman, B. *Rubberlike Elasticity A Molecular Primer*; Wiley: New York, 1988.000
(18) Pearson, D. S. *Macromolecules* **1977**, *10*, 696–701.
(19) Tanaka, T.; Hocker, L. O.; Benedek, G. B. *J. Chem. Phys.* **1973**, *59*, 5151–5159.
(20) Einstein, A. Theory of the opalescence of homogeneous liquids and mixtures of liquids in the vicinity of the critical state. In *Colliod chemistry*; Alexander, J., Ed.; Reinhold: New York, 1926; Vol. 1, p 323.
(21) Zimm, B. H. *J. Chem. Phys.* **1948**, *16*, 1093–1099.
(22) Higgins, J. S.; Benoit, H. C. *Polymers and Neutron Scattering*; Clarendon Press: Oxford, U.K., 1994.000
(23) Benoit, H. *J. Polym. Sci.* **1953**, *11*, 507–510.
(24) Richter, D.; Farago, B.; Huang, J. S.; Fetters, L. J.; Ewen, B. *Macromoleules* **1989**, *22*, 468–472.
(25) Ornstein, L. S.; Zernike, F. *Proc. Acad. Sci., Amsterdam* **1914**, *17*, 793.
(26) Shibayama, M. *Macromol. Chem. Phys.* **1998**, *199*, 1–30.
(27) Shibayama, M.; Isono, K.; Okabe, S.; Karino, T.; Nagao, M. *Macromolecules* **2004**, *37*, 2909–2918.
(28) Okabe, S.; Nagao, M.; Karino, T.; Watanabe, S.; Adachi, T.; Shimizu, H.; Shibayama, M. *J. Appl. Crystallogr.* **2005**, *38*, 1035–1037.
(29) Okabe, S.; Karino, T.; Nagao, M.; Watanabe, S.; Shibayama, M. *Nucl. Inst. Methods Phys. Res., A* **2007**, *572*, 853–858.
(30) Shibayama, M.; Nagao, M.; Okabe, S.; Karino, T. *J. Phys. Soc. Jpn.* **2005**, *74*, 2728–2736.
(31) Hedden, R. C.; Saxena, H.; Cohen, C. *Macromolecules* **2000**, *33*, 8676–8684.
(32) Mallam, S.; Horkay, F.; Hecht, A. M.; Geissler, E. *Macromolecules* **1989**, *22*, 3356.
(33) Horkay, F.; Tasaki, I.; Basser, P. J. *Biomacromolecules* **2000**, *1*, 84–90.
(34) Lutolf, M. P.; Hubbell, J. A. *Biomacromolecules* **2003**, *4*, 713–722.
(35) Debye, P.; Bueche, A. M. *J. Chem. Phys.* **1950**, *18*, 1423–1425.
(36) Soni, V. K.; Stein, R. S. *Macromolecules* **1990**, *23*, 5257–5265.
(37) Brandrup, J.; Immergut, E. H. *Polymer Handbook*; Wiley Interscience: New York, 1989.000
(38) Burchard, W. *Adv. Polym. Sci.* **1999**, *143*, 115–194.
(39) de Gennes, P. G. *Scaling Concepts in Polymer Physics*; Cornell University: Ithaca, NY, 1979.000
(40) Shibayama, M.; Takahashi, H.; Nomura, S. *Macromolecules* **1995**, *28*, 6860–6864.
(41) Bastide, J.; Leibler, L. *Macromolecules* **1988**, *21*, 2647.

MA802280N